Search for Fractionally Charged Particles with CUORE

D. Q. Adams, ¹ C. Alduino, ¹ K. Alfonso, ² F. T. Avignone III, ¹ O. Azzolini, ³ G. Bari, ⁴ F. Bellini, ^{5,6} G. Benato, ^{7,8} M. Beretta, ⁹ M. Biassoni, ¹⁰ A. Branca, ^{11,10} C. Brofferio, ^{11,12} C. Bucci, ⁸ J. Camilleri, ² A. Caminata, ¹³ A. Campani, ^{14,13} J. Cao, ¹⁵ S. Capelli, ^{11,12} C. Capelli, ⁸ L. Cardani, ¹⁷ P. Carniti, ^{11,12} N. Casali, ¹⁷ E. Celi, ^{7,18} D. Chiesa, ^{11,12} M. Clemenza, ¹² S. Copello, ¹⁹ O. Cremonesi, ¹² R. J. Creswick, ¹ A. D'Addabbo, ¹⁸ I. Dafinei, ¹⁷ F. Del Corso, ^{20,21} S. Dell'Oro, ^{11,12} S. Di Domizio, ^{14,13} S. Di Lorenzo, ¹⁸ T. Dixon, ²² V. Dompè, ^{5,17} D. Q. Fang, ¹⁵ G. Fantini, ^{5,17} M. Faverzani, ^{11,12} E. Ferri, ¹² F. Ferroni, ^{7,17} E. Fiorini, ^{11,12} M. A. Franceschi, ²³ S. J. Freedman, ^{16,9,*} S. H. Fu, ^{15,18} B. K. Fujikawa, ¹⁶ S. Ghislandi, ^{7,18} A. Giachero, ^{11,12} M. Girola, ¹¹ L. Gironi, ^{11,12} A. Giuliani, ²² P. Gorla, ¹⁸ C. Gotti, ¹² P. V. Guillaumon, ^{18,†} T. D. Gutierrez, ²⁴ K. Han, ²⁵ E. V. Hansen, ⁹ K. M. Heeger, ²⁶ D. L. Helis, ^{7,18} H. Z. Huang, ²⁷ G. Keppel, ²⁸ Yu. G. Kolomensky, ^{9,16} R. Kowalski, ²⁹ R. Liu, ²⁶ L. Ma, ^{15,27} Y. G. Ma, ¹⁵ L. Marini, ^{7,18} R. H. Maruyama, ²⁶ D. Mayer, ³⁰ Y. Mei, ¹⁶ M. N. Moore, ²⁶ T. Napolitano, ²³ M. Nastasi, ^{11,12} C. Nones, ³¹ E. B. Norman, ³² A. Nucciotti, ^{11,12} I. Nutini, ¹² T. O'Donnell, ² M. Olmi, ¹⁸ B. T. Oregui, ²⁹ J. L. Ouellet, ³⁰ S. Pagan, ²⁶ C. E. Pagliarone, ^{18,33} L. Pagnanini, ^{7,18} M. Pallavicini, ^{14,13} L. Pattavina, ¹⁸ M. Pavan, ^{11,12} G. Pessina, ¹² V. Pettinacci, ¹⁷ C. Pira, ²⁸ S. Pirro, ¹⁸ E. G. Pottebaum, ²⁶ S. Pozzi, ^{12,11} E. Previtali, ^{11,12} A. Puiu, ¹⁸ S. Quitadamo, ^{7,18} A. Ressa, ^{5,17} C. Rosenfeld, ¹ B. Schmidt, ³¹ V. Sharma, ² V. Singh, ⁹ M. Sisti, ¹² D. Speller, ²⁹ P. Stark, ³⁰ P. T. Surukuchi, ³⁴ L. Taffarello, ³⁵ C. Tomei, ¹⁷ A. Torres, ² J. A. Torres, ²⁶ K. J. Vetter, ^{9,16} M. Vignati, ^{5,17} S. L. Wagaarachchi, ^{9,}

(CUORE Collaboration)

```
<sup>1</sup>Department of Physics and Astronomy, University of South Carolina, Columbia, SC 29208, USA
        <sup>2</sup>Center for Neutrino Physics, Virginia Polytechnic Institute and State University, Blacksburg, Virginia 24061, USA
                              <sup>3</sup>INFN—Laboratori Nazionali di Legnaro, Legnaro (Padova) I-35020, Italy
                                          <sup>4</sup>INFN—Sezione di Bologna, Bologna I-40127, Italy
                             <sup>5</sup>Dipartimento di Fisica, Sapienza Università di Roma, Roma I-00185, Italy
                                             <sup>6</sup>INFN—Sezione di Roma, Roma I-00185, Italy
                                         <sup>7</sup>Gran Sasso Science Institute, L'Aquila I-67100, Italy
                           <sup>8</sup>INFN—Laboratori Nazionali del Gran Sasso, Assergi (L'Aquila) I-67100, Italy
                              Department of Physics, University of California, Berkeley, CA 94720, USA
                                       <sup>10</sup>INFN—Sezione di Milano Bicocca, Milano I-20126, Italy
                            <sup>11</sup>Dipartimento di Fisica, Università di Milano-Bicocca, Milano I-20126, Italy
                                       <sup>12</sup>INFN—Sezione di Milano Bicocca, Milano I-20126, Italy
                                           <sup>13</sup>INFN—Sezione di Genova, Genova I-16146, Italy
                                <sup>14</sup>Dipartimento di Fisica, Università di Genova, Genova I-16146, Italy
                <sup>15</sup>Key Laboratory of Nuclear Physics and Ion-beam Application (MOE), Institute of Modern Physics,
                                              Fudan University, Shanghai 200433, China
                  <sup>16</sup>Nuclear Science Division, Lawrence Berkeley National Laboratory, Berkeley, CA 94720, USA
                                             <sup>17</sup>INFN—Sezione di Roma, Roma I-00185, Italy
                           <sup>18</sup>INFN—Laboratori Nazionali del Gran Sasso, Assergi (L'Aquila) I-67100, Italy
                                             <sup>19</sup>INFN—Sezione di Pavia, Pavia I-27100, Italy
          <sup>20</sup>Dipartimento di Fisica e Astronomia, Alma Mater Studiorum—Università di Bologna, Bologna I-40127, Italy
                                          <sup>21</sup>INFN—Sezione di Bologna, Bologna I-40127, Italy
                                <sup>22</sup>Université Paris-Saclay, CNRS/IN2P3, IJCLab, 91405 Orsay, France
                              <sup>23</sup>INFN—Laboratori Nazionali di Frascati, Frascati (Roma) I-00044, Italy
                 <sup>24</sup>Physics Department, California Polytechnic State University, San Luis Obispo, CA 93407, USA
 <sup>25</sup>INPAC and School of Physics and Astronomy, Shanghai Jiao Tong University; Shanghai Laboratory for Particle Physics and
                                                  Cosmology, Shanghai 200240, China
                     <sup>26</sup>Wright Laboratory, Department of Physics, Yale University, New Haven, CT 06520, USA
                  <sup>27</sup>Department of Physics and Astronomy, University of California, Los Angeles, CA 90095, USA
                             <sup>28</sup>INFN—Laboratori Nazionali di Legnaro, Legnaro (Padova) I-35020, Italy
   <sup>29</sup>Department of Physics and Astronomy, The Johns Hopkins University, 3400 North Charles Street Baltimore, MD, 21211
                                 <sup>30</sup>Massachusetts Institute of Technology, Cambridge, MA 02139, USA
                                <sup>31</sup>IRFU, CEA, Université Paris-Saclay, F-91191 Gif-sur-Yvette, France
                     <sup>32</sup>Department of Nuclear Engineering, University of California, Berkeley, CA 94720, USA
<sup>33</sup>Dipartimento di Ingegneria Civile e Meccanica, Università degli Studi di Cassino e del Lazio Meridionale, Cassino I-03043, Italy
```

Department of Physics and Astronomy, University of Pittsburgh, Pittsburgh, PA 15260, USA
 INFN—Sezione di Padova, Padova I-35131, Italy
 Engineering Division, Lawrence Berkeley National Laboratory, Berkeley, CA 94720, USA

(Received 18 June 2024; revised 25 September 2024; accepted 22 October 2024; published 12 December 2024)

The Cryogenic Underground Observatory for Rare Events (CUORE) is a detector array comprised by 988 5 cm \times 5 cm \times 5 cm \times 5 cm TeO₂ crystals held below 20 mK, primarily searching for neutrinoless double-beta decay in ¹³⁰Te. Unprecedented in size among cryogenic calorimetric experiments, CUORE provides a promising setting for the study of exotic throughgoing particles. Using the first tonne year of CUORE's exposure, we perform a search for hypothesized *fractionally charged particles* (FCPs), which are well-motivated by various standard model extensions and would have suppressed interactions with matter. Across the searched range of charges e/24 - e/2 no excess of FCP candidate tracks is observed over background, setting leading limits on the underground FCP flux with charges e/24 - e/5 at 90% confidence level. Using the low background environment and segmented geometry of CUORE, we establish the sensitivity of tonne-scale subkelvin detectors to diverse signatures of new physics.

DOI: 10.1103/PhysRevLett.133.241801

Charge quantization remains an unsolved mystery of the standard model (SM). Since the measurement of the electron charge quantum e by Millikan and Fletcher [1], the charges of all known elementary particles have been empirically found to follow a simple rule: their charges are all either zero, $\pm e$, $\pm \frac{1}{3}e$, or $\pm \frac{2}{3}e$. Of these, only particles with integer electron charges $(q = ne \text{ for } n = 0, \pm 1)$ have been observed as free particles [2].

Yet, there is no *a priori* reason that the charge must be quantized. Existing explanations, such as Dirac quantization through magnetic monopoles [3] or grand unified theories (GUTs) [2], are yet to be confirmed, and the everexpanding theoretical landscape has introduced many promising extensions to the standard model that permit free fractionally charged particles (FCPs). These candidates can arise from theories with nonstandard charge quantization [4,5], hidden sector couplings to vector bosons [6], or additional gauge groups [7–9] and may appear in the form of unbound quarks [10,11] or novel leptons [12,13].

Fractionally charged particles (also known as *lightly ionizing* particles or *millicharged* particles when $q \ll e$) are parameterized by charge q = e/f with f > 1 and would present distinct experimental signatures due to their suppressed ionization energy losses relative to known charged particles. FCPs have been the subject of an extensive experimental effort over the past several decades [14], spanning particle accelerators [15–17], balloon and space

Published by the American Physical Society under the terms of the Creative Commons Attribution 4.0 International license. Further distribution of this work must maintain attribution to the author(s) and the published article's title, journal citation, and DOI. Funded by SCOAP³. satellite experiments [18,19], and bulk matter searches [20,21].

Low-background underground detectors may be used to search for FCPs possibly present within the flux of cosmic rays by looking for interaction signatures from FCPs crossing a passive detector. Such direct detection searches are frequently model independent and inclusive across possible production mechanisms, such as electromagnetic decays of mesons [22], Drell-Yan processes of primary cosmic rays with the Earth's atmosphere [23], or as boosted relics within the primary cosmic ray flux [24]. In this Letter, we report on a search for an underground flux of relativistic fractionally charged particles in the range f=2–24 with the Cryogenic Underground Observatory for Rare Events (CUORE) experiment.

CUORE is a tonne-scale millikelvin experiment located underground at the Laboratori Nazionali del Gran Sasso (LNGS) in Italy, with the primary purpose of searching for neutrinoless double beta decay $(0\nu\beta\beta)$ in ¹³⁰Te [25]. The experiment consists of an array of 5 cm × 5 cm × 5 cm TeO₂ crystals held below 20 mK within the CUORE cryostat [26]. Each crystal detector is coupled to a neutron transmutation doped germanium thermistor to read out thermal pulses produced by energy depositions in the crystal [27].

CUORE's highly segmented geometry, comprised of 988 crystal detectors arranged in 19 four-column vertical towers of 13 crystals each, aids background rejection for $0\nu\beta\beta$ searches through anticoincidence between channels [25] and has been used to search for rare nuclear decays of ¹²⁰Te and ¹³⁰Te with signatures distributed over two to three crystals [28,29]. We extend CUORE's capability to reconstruct detectorwide signatures of new physics, and establish that cryogenic bolometric detectors have reached sufficient scale to reconstruct through-going particle tracks.

FCPs would interact with CUORE primarily through ionization energy loss, leaving linear tracks across multiple

Deceased.

[†]Present address: Instituto de Física, Universidade de São Paulo, São Paulo 05508-090, Brazil.

crystals in the detector. The stopping power is fainter than a q = e minimally ionizing particle, leaving a distinct signature of new physics. Similar to the treatment in [30], the flux $\Phi(f)$ of FCPs through the detector may be expressed as

$$\Phi(f) = \frac{n^{\text{Sig}}}{T_{\text{livetime}} \cdot (A\Omega)_{\text{selection}} \cdot \epsilon_{\text{cluster}}}, \quad (1)$$

where n^{Sig} is the total number of signal candidates (observed or undetected limits), $(A\Omega)_{\mathrm{selection}}$ is CUORE's acceptance to FCPs coming from the inherent detector physics, geometry, and analysis selections, $\epsilon_{\mathrm{cluster}}$ is a global efficiency term from the probability of successfully temporally clustering together all detector events induced by an FCP, and T_{livetime} is the total detector livetime of the search. Values for n^{Sig} and $(A\Omega)_{\mathrm{selection}}$ will generally be f dependent.

Methods and data selection-Physics data collected in CUORE are grouped into datasets with one to two month duration, bookended by the deployment of calibration sources about the detector. For this search, we use the first tonne year of CUORE's exposure as described in [31] collected over 15 datasets. We remove periods of time characterized by the anomalously high occurrence of lowenergy pulses in the detector believed to be nonparticle in origin. Such events appear to arise from correlated noise on multiple detector channels, combined with pulse-cleaning selections loosening at low energies. Methods for their efficient rejection are under further development. For searches in CUORE for signal signatures occurring in one or few crystals (such as $0\nu\beta\beta$), such periods can be excluded on a channel-wise basis to avoid losing exposure from channels which are operating nominally. This search targets broad detectorwide signatures across many crystals, thus we conservatively remove the entirety of a datacollection interval (with typical duration of 24 hours) should it be found to contain a contaminated period. Altogether, this rejects 20.3% of the analyzed exposure, and after such removal this search considers a total exposure of 442.3 days of detector live time.

We refer to reconstructed energy depositions within any given crystal as *events*, and multiple events occurring concurrently within the detector as a *cluster*. Events are triggered offline from continuously collected detector time streams, which are then filtered for amplitude and energy estimation with methods described in [31]. For this analysis, we consider events with reconstructed energies between 20 keV and 6 MeV per crystal. This energy range is set by detector trigger thresholds at the lower end, and to avoid overlap with energy depositions from throughgoing muons at the higher end, translating to sensitivity for *f* values between 2 and 24.

We apply pulse-shape cuts using principal component analysis to reduce nonphysical events and those with poor pulse reconstruction [31]. We build clusters by grouping temporally related events with a boxcar filter and identify clusters containing six or more contemporaneous events. We denote the number of events in a given cluster as the cluster *multiplicity*, \mathcal{M} , corresponding to the number of crystals triggered in coincidence with each other. The filter window is tuned using estimates of CUORE's timing resolution derived from the interarrival time distribution of events within the detector. Selecting 80 ms, we find a detectorwide clustering efficiency of $\epsilon_{\text{cluster}} = 94(1)\%$ for $\mathcal{M} \geq 6$ events.

Cosmic ray muons present a potential background to any linear track search in CUORE and are expected to register in the detector with per-crystal energy depositions of $\mathcal{O}(10-50 \text{ MeV})$. Such events may saturate the dynamic range of our readout electronics [32] above 15 MeV, hindering accurate energy estimation. We veto against muon events by discarding clusters in coincidence with any saturated event or event greater than 10 MeV in energy. From Monte Carlo simulations of expected muon backgrounds, we find this self-veto criterion to be more than 99.9% efficient at rejecting muons which directly pass through two or more crystals within the detector array. We additionally find that occasional thermal, vibrational, or microphonic noise can produce manifestly colinear correlated events on a single detector column. We therefore reject clusters with at least 60% of channels occurring within the same column. This single-column-fraction cut reduces CUORE's analysis acceptance by up to 6% assuming a half-isotropic flux of FCPs or up to 19% assuming a steeper angular flux equal to that exhibited by muons within LNGS [33].

Clusters passing these selections are then fit with a version of the multiobjective optimization (MOO) algorithm presented in [34] tailored to FCP reconstruction. We utilize both the spatial arrangement of a cluster along with the distribution of measured energy-depositions to search for faintly-ionizing tracklike clusters which are expected should a relativistic FCP cross the detector.

Fitting a track to a cluster of events within CUORE gives rise to two track consistency parameters: the number of *extra* channels that are intersected by the fitted track but do not register an event and the number of *missing* channels that register energy but are not intersected by the fitted track. Clusters with low numbers of extra channels and missing channels (referred to as ExtraCh and MissingCh, respectively) are more indicative of a throughgoing particle track. Examples clusters and corresponding fitted tracks are shown in Fig. 1.

We modify the MOO algorithm to provide for each fitted cluster a maximum-likelihood estimate of the f value which is most consistent with the observed pattern of energy deposition along the best-fit track. For each event within a cluster, we use the measured energy, ΔE , and reconstructed path length through the corresponding crystal, Δx , to determine the inferred stopping power, $\Delta E/\Delta x$. We then obtain from the inferred stopping powers the

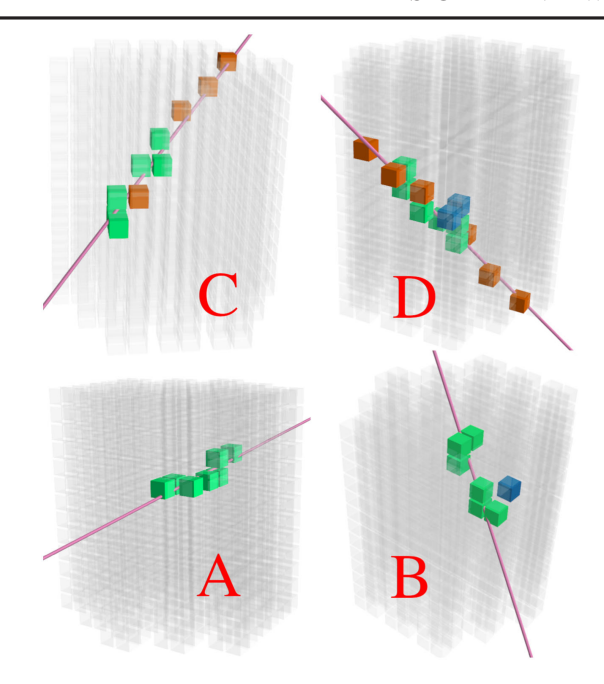


FIG. 1. Four example track-fit clusters observed in data as they appear within the CUORE detector array. The best-fit tracks are shown in purple, while channels which are both intersected by the best-fit track and register an event are shown in green. "Missing" channels corresponding to channels which register an event but are not intersected by the best-fit track are shown in blue, while "extra" channels which are intersected by the best-fit track without a corresponding observed event are shown in red. Channels which are nonparticipating in the cluster or track fit thereof are shown translucently. The four example tracks (A, B, C, D) are each representative of the ABCD categorizations based on the presence or absence of extra and missing channels exhibited by the fitted cluster topology, as used in the present analysis.

corresponding f value most likely to produce that cluster, assuming minimally-ionizing FCPs. Both extra channels (for which $\Delta E = 0$) and missing channels (which have $\Delta x = 0$) are excluded from this estimate.

This enables us to directly search for an excess in the distribution of reconstructed f arising from track-fitting selected clusters, as would be induced by a population of FCPs within the underground cosmic ray flux. From each fitted cluster, we extract the tuple of fitted observables: (f, ExtraCh, MissingCh).

The ExtraCh and MissingCh track consistency parameters also provide the means to statistically constrain search backgrounds from non-tracklike clusters. Background processes capable of depositing energy across several crystals include naturally-occurring or trace radio-nuclides which produce MeV-scale γ rays or multiple interacting final state particles within their decay radiation, such as 40 K, 60 Co, and 214 Bi. Other background sources include cosmic ray muons which do not directly intersect detector crystals but do clip shielding layers producing electromagnetic shower products with high event

multiplicity and γ -ray deexcitation cascades from neutron captures on detector components producing clusters with total energies up to 10 MeV. Accidental pileup of two lower-multiplicity clusters will also contribute to the search background. Background clusters exhibit elevated distributions of ExtraCh and MissingCh counts as compared to FCP signal candidates.

FCP signals are simulated by incorporating the package developed by S. Banik and others [35] into CUORE's GEANT4 [36–38] Monte Carlo (MC) detector model. The simulation treats FCPs as massive fermions with relevant electromagnetic loss processes correspondingly suppressed. We nominally consider a minimally-ionizing relativistic particle ($\beta \gamma = 3$) of mass 100 GeV/ c^2 but find that we are insensitive to differences in particle mass over the range of 100 MeV/ c^2 -1 TeV/ c^2 and relativistic parameters $\beta \gamma = 3$ –300. We simulate FCPs at eight logarithmically-spaced charge values f = 2–24, sampled uniformly across a 15 meter radius disk centered above the detector, covering angles up to 5 degrees from horizontal.

Per dataset, we tune the output of these simulations to match detection inefficiencies as exhibited within the collected data, which can impact cluster reconstruction. We mimic channelwise dead time within the detector, reflecting when particular channels are not taking good physics data. We determine trigger probabilities with the synthetic data method presented in [39], which may be less than unity for energies below ~40 keV. Additionally, we consider a base-cut efficiency for whether an event will be well-reconstructed and free from pileup within the event window, as in [31]. Finally, we consider the event selection efficiency for pulse-cleaning cuts. Above 100 keV, we use the technique described in [40] by counting the fraction of events within known γ and α peaks passing and failing cuts. Below 100 keV, we determine our event selection efficiency using low-energy events arising from high-multiplicity electromagnetic cascades found in coincidence with throughgoing muon candidates.

From the efficiency-tuned MC output and implementing all clusterwise cuts as applied to data, we determine the area \times solid-angle geometric acceptance, $(A\Omega)$, of CUORE to isotropically downward-going FCPs, displayed in Fig. 2. Alternatively, if FCPs are assumed to follow a muonlike angular distribution within LNGS [41], these acceptance values are reduced by up to 50%, reflecting the lower geometric and analysis acceptance of CUORE to a more downward-going muonlike flux. We consider the halfisotropic and muonlike angular distributions to respectively provide minimally- and maximally-attenuated limiting cases for how a relativistic flux of FCPs may appear underground after passing through the mountain overburden to reach CUORE. In general, relating an underground flux of FCPs to that on the Earth's surface will depend on particle parameters along with their supposed production mechanism.

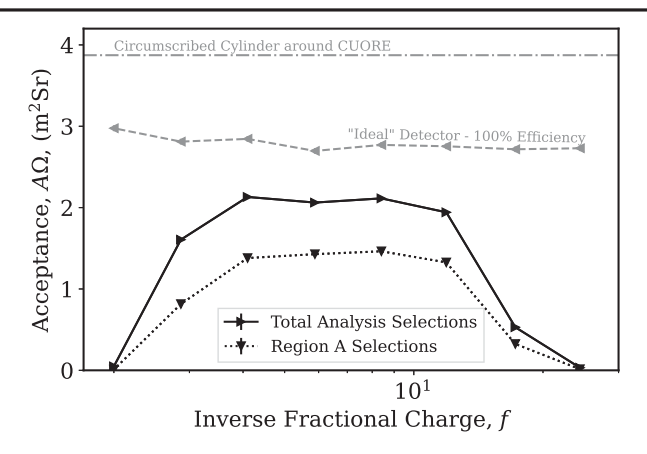


FIG. 2. Acceptance of CUORE to isotropically downward-going FCPs, from Monte Carlo simulations of FCP interactions with the detector. Shown is the total acceptance after all cuts entering into the ABCD template selections (solid black), along with the portion coming from clusters within Region A (dashed black). The falloff at high/low f values reflects typical FCP energy depositions falling outside the 20 keV–6 MeV analysis selections of this search. Values are also shown for a reference cylinder circumscribed around the CUORE detector (dot-dashed gray), along with CUORE's acceptance to $\mathcal{M} \geq 6$ clusters under idealistic conditions, i.e., assuming 100% detection efficiency and without analysis selections on event energy (dashed gray).

Results—This search takes a data-driven approach to background estimation, using the ABCD method [42] commonly employed for analyses at collider experiments (see for example [43–45]). This technique leverages that the distributions of ExtraCh and MissingCh are found to be statistically independent for background events arising from non-tracklike sources, while being highly correlated and suppressed in number for clusters induced by FCPs.

We bin fitted clusters by f value into three bins logarithmically-spaced f=1–40 and additionally define ABCD regions by the binary cuts in the number of extra and missing channels as shown by the solid divisions and labeling in Fig. 3 and utilize the following likelihood model to fit to both data and toy experiments:

$$-2\log \mathcal{L} = \sum_{i \in f \text{ bins } j \in \{A,B,C,D\}} -2\log \operatorname{Pois}(k_{ij}; N_{ij}), \qquad (2)$$

where

$$\begin{split} N_{iA} &= \epsilon_{iA} n^{\mathrm{Sig}} + n_{i}^{\mathrm{Bgd}}, \\ N_{iB} &= \epsilon_{iB} n^{\mathrm{Sig}} + \tau_{iB} n_{i}^{\mathrm{Bgd}}, \\ N_{iC} &= \epsilon_{iC} n^{\mathrm{Sig}} + \tau_{iC} n_{i}^{\mathrm{Bgd}}, \\ N_{iD} &= \epsilon_{iD} n^{\mathrm{Sig}} + \tau_{iB} \tau_{iC} n_{i}^{\mathrm{Bgd}}. \end{split} \tag{3}$$

Here, k_{ij} are the observed data in f-bin i and region j, n^{Sig} is our parameter of interest for the total number of signal

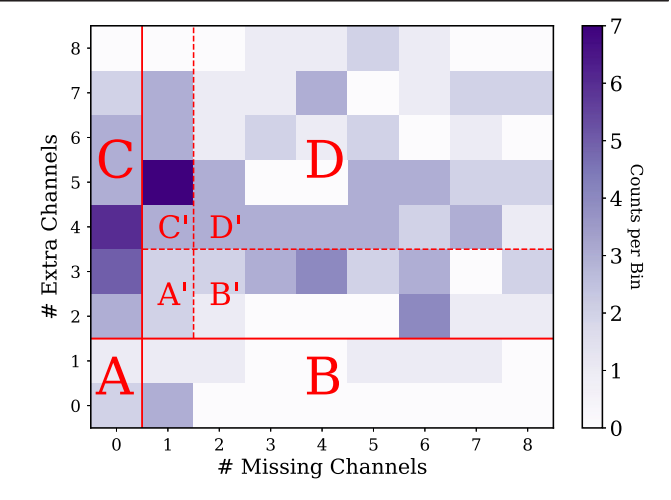


FIG. 3. Observed clusters within the search data after applying analysis selections, binned onto the plane of the number of missing channels (MissingCh) and extra channels (ExtraCh) arising from track fitting. The selected ABCD regions are marked by solid red lines, while the validation ABCD subdivisions of Region D are marked by dashed red lines.

events, ϵ_{ij} are normalized signal templates from our efficiency-tuned FCP MC simulations, while $n_i^{\rm Bgd}$, τ_{iB} , and τ_{iC} are f-bin specific background nuisance parameters encoding the ABCD behavior into the model. Fitting is performed with the iminuit implementation [46] of the Minuit algorithm [47].

To reflect the degradation of signal candidate clusters due to accidental coincidences with uncorrelated background events within the detector, we move a corresponding 4.5% of template weight from Region A to Region B and from Region C to Region D. Given our clustering method and selections, this reflects the probability of detectorwide pileup with an uncorrelated event, which can induce one or more additional missing channels when the resulting cluster is track fit.

We perform our analysis with gradual unblinding of clusters within data. We start with the unblinding of clusters in Region D for model validation. Then we make available clusters within Region B and C for pre-unblinding sensitivity studies, and finally we unblind Region A with the analysis finalized.

We validate the ABCD model by examining Region D, which we expect to be comprised nearly entirely by background clusters. We further subdivide Region D into four validation inset regions as shown in Fig. 3. We fit the validation regions to a background-only ABCD model and compare the result with fits to toy experiments drawn from the best-fit background parameters for the validation region. We find that the fitted value of $-2 \log \mathcal{L}$ lies in the 70^{th} quantile of the sampling distribution from toy experiments, indicating good agreement between the ABCD model and the observed validation region. Additionally, a Pearson-r test [48] to data within Region

D does not show evidence of correlation between the ExtraCh and MissingCh observables with an r coefficient of -0.04 at p=0.58, further supporting the use of the ABCD model to describe background clusters.

We use a frequentist profile-likelihood ratio statistic to test between background-only and background-plus-FCP hypotheses [49]. We repeat this test at each simulated f value separately and derive global test significances as corrected by a numerically-determined trial factor of 3.8 to account for the look-elsewhere effect [50]. Since our data is in a low-statistics regime, we cannot rely on asymptotic approximations [51] and instead build sampling distributions from toy experiments to determine test-statistic thresholds and confidence brackets.

In constructing toy experiments, we vary background nuisance parameters according to the hybrid *a posteriori* Highland-Cousins technique [52]. We determine a multivariate normal (MVN) distribution for our background nuisance parameters from fits to the observed data salted with additional signal counts. For each toy experiment, we sample the MVN distribution to determine nuisance parameter values and then Poisson sample the resulting background template to obtain a toy background spectrum. Toy experiments with nonzero injected signal counts sample FCP signal templates accounting for inherent Poisson fluctuations, and the additional variance from finite Monte Carlo statistics.

Fitting to the observed data, we find no evidence for an excess of FCP-induced tracks and find that the data is welldescribed by background-only fits across all tested values of f. Likelihood ratio test statistic values do not exceed 1σ local (or global) significance in favor of FCPs across the values tested. The observed data, along with our best-fit ABCD reconstruction and signal exclusion at f = 4.1, are shown in Fig. 4. We proceed to set upper limits at 90% confidence level on the observed number of signal counts using brackets built from fits to toy experiments using a two-sided Neyman construction with Feldman-Cousins ordering [51,53]. We prevent ourselves from making exclusions stronger than would be made under an observation of zero signal counts with the method of Lokhov and Tkachov [54]. We convert these f-dependent exclusions, which range between 5.1 and 8.3 signal counts, into limits on the underground flux of FCPs using Eq. (1), which we display in Fig. 5 for a half-isotropic downward angular distribution.

We find that these limits are world leading among underground experiments for the range of inverse fractional charges between f=5–24 with a minimum exclusion of $\Phi < 6.9 \times 10^{-12} \ \mathrm{cm^{-2}} \ \mathrm{s^{-1}} \ \mathrm{Sr^{-1}}$ (90% C.L.) at f=11.9, bridging a gap between historical general-purpose large-volume underground detectors [55–57] and more contemporary searches targeting smaller charge values with reduced detector exposures [30,58]. Over this range of possible charges, collider and beam-dump exclusions constrain FCPs up to masses of 1–4.7 GeV/ c^2 [15,17], while other recent limits from the energy frontier extend up to

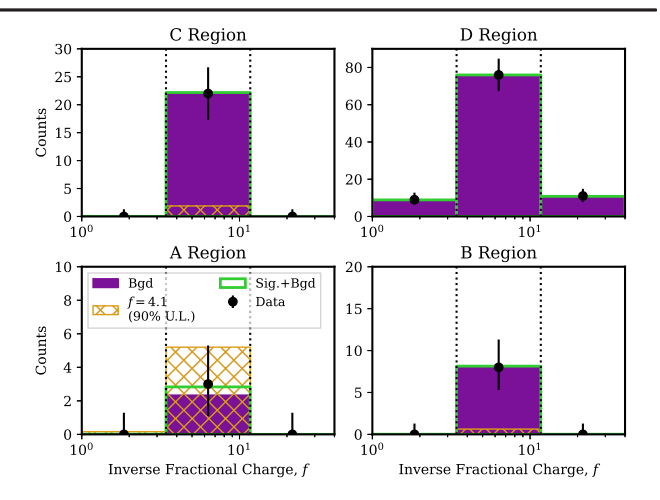


FIG. 4. Observed cluster counts, binned by reconstructed f-value and ABCD subdivisions of ExtraCh and MissingCh. We also show the background-plus-FCPs best fit to the data for f=4.1, compatible within 1σ with the absence of a signal. Displayed are the best-fit background component (solid purple), total signal-plus-background fit (green line), along with the signal template corresponding to the excluded 90% upper limit of 8.3 signal counts (hashed orange). Clusters induced by one or more naturally-occurring γ rays multiple scattering within the detector typically reconstruct within the central bin, contributing to elevated background counts as compared to the two side bins of the search.

100–600 GeV/ c^2 but only for the range $f \leq 3$ [16]. Bulkmatter searches for FCPs bound to normal matter have probed smaller charge values than those considered in this search, including into the f > 1000 millicharged regime

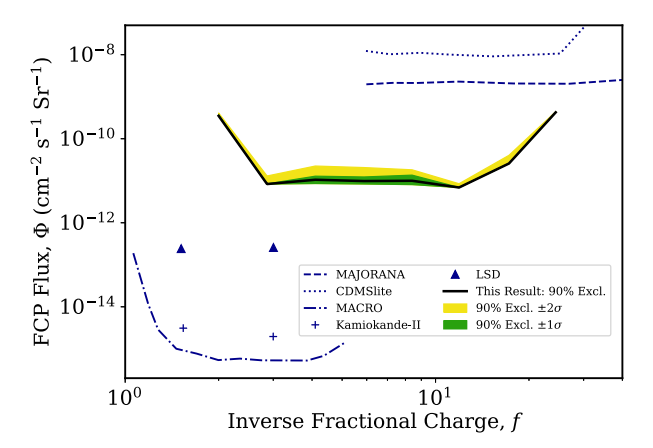


FIG. 5. Observed exclusions at 90% C.L. on the underground flux of FCPs as a function of inverse fractional charge, assuming a half-isotropic downward-going angular distribution. Also shown are the $\pm 1\sigma$ and $\pm 2\sigma$ ranges of expected exclusions under the background-only hypothesis, as derived from toy experiments. Assuming an alternative muonlike angular distribution yields flux limits and expected ranges up to 2 times weaker than those presented. We compare with published underground limits from other experiments [30,55–58].

[21]. Such experiments are sensitive to the production mechanism or hypothesized relic abundance of FCPs, along with the material history of samples used within a search [14], and their corresponding results are difficult to compare directly with underground flux limits.

Conclusion—This search establishes new limits on the underground FCP flux, carving out significant new space across inverse charge parameters for relativistic particle species possibly present within cosmic radiation underground. More broadly, we demonstrate CUORE's capability to search for exotic detectorwide signatures of new physics. Analysis and processing techniques are under development to extend analysis thresholds and efficiencies in CUORE to lower energies, which would provide sensitivity to fractional charges more feebly interacting than those examined in this Letter. Similar searches in the forthcoming CUPID experiment [59] will benefit from finer detector segmentation and additional detector information provided by the dual readout of heat and light signatures.

This Letter makes use of both the DIANA data analysis and APOLLO data acquisition software packages, which were developed by the CUORICINO, CUORE, LUCIFER, and CUPID-0 Collaborations.

Acknowledgments—The CUORE Collaboration thanks the directors and staff of the Laboratori Nazionali del Gran Sasso and the technical staff of our laboratories. This work was supported by the Istituto Nazionale di Fisica Nucleare (INFN); the National Science Foundation under Grant Nos. NSF-PHY-0605119, NSF-PHY-0500337, NSF-PHY-0855314, NSF-PHY-0902171, NSF-PHY-0969852, NSF-PHY-1307204, NSF-PHY-1314881, 1401832, and NSF-PHY-1913374; Yale University, Johns Hopkins University, and the University of Pittsburgh. This material is also based upon work supported by the US Department of Energy (DOE) Office of Science under Contract No. DE-AC02-05CH11231 and No. DE-AC52-07NA27344; by the DOE Office of Science, Office of Nuclear Physics, under Contract No. DE-FG02-08ER41551, No. DE-FG03-00ER41138, No. DE-SC0012654, No. DE-SC0020423, No. DE-SC0019316, and No. DE-SC0011091. This research used resources of the National Energy Research Scientific Computing Center (NERSC). The authors acknowledge Advanced Research Computing at Virginia Tech University for providing computational resources and technical support that have contributed to the results reported within this Letter.

- [3] P. Dirac, Quantised singularities in the electromagnetic field, Proc. R. Soc. London, Ser. A 133, 60 (1931).
- [4] K. S. Babu and R. N. Mohapatra, Quantization of electric charge from anomaly constraints and a Majorana neutrino, Phys. Rev. D 41, 271 (1990).
- [5] A. Ignatiev, V. Kuzmin, and M. Shaposhnikov, Is the electric charge conserved?, Phys. Lett. **84B**, 315 (1979).
- [6] E. Izaguirre and I. Yavin, New window to millicharged particles at the LHC, Phys. Rev. D **92**, 035014 (2015).
- [7] P. H. Frampton and T. W. Kephart, Fractionally charged particles as evidence for supersymmetry, Phys. Rev. Lett. 49, 1310 (1982).
- [8] B. Holdom, Two U(1)'s and ϵ charge shifts, Phys. Lett. **166B**, 196 (1986).
- [9] B. Holdom, Searching for ϵ charges and a new U(1), Phys. Lett. B **178**, 65 (1986).
- [10] L. Lyons, Quark search experiments at accelerators and in cosmic rays, Phys. Rep. 129, 225 (1985).
- [11] L. Lyons, Current status of quark search experiments, Prog. Part. Nucl. Phys. 7, 157 (1981).
- [12] E. Chun, A. S. Joshipura, and A. Smirnov, Models of light singlet fermion and neutrino phenomenology, Phys. Lett. B 357, 608 (1995).
- [13] C. Kouvaris, Composite millicharged dark matter, Phys. Rev. D 88, 015001 (2013).
- [14] M. L. Perl *et al.*, Searches for fractionally charged particles, Annu. Rev. Nucl. Part. Sci. 59, 47 (2009).
- [15] A. Ball *et al.*, Search for millicharged particles in protonproton collisions at $\sqrt{s} = 13$ TeV, Phys. Rev. D **102**, 032002 (2020).
- [16] T. Aarrestad *et al.* (CMS Collaboration), Search for fractionally charged particles in proton-proton collisions at $\sqrt{s} = 13$ TeV, arXiv:2402.09932.
- [17] R. Acciarri *et al.* (ArgoNeuT Collaboration), Improved limits on millicharged particles using the argoneut experiment at Fermilab, Phys. Rev. Lett. **124**, 131801 (2020).
- [18] H. Fuke *et al.*, Search for fractionally charged particles in cosmic rays with the BESS spectrometer, Adv. Space Res. **41**, 2050 (2008).
- [19] F. Alemanno *et al.* (DAMPE Collaboration), Search for relativistic fractionally charged particles in space, Phys. Rev. D **106**, 063026 (2022).
- [20] M. Pospelov and H. Ramani, Earth-bound millicharge relics, Phys. Rev. D **103**, 115031 (2021).
- [21] G. Afek, F. Monteiro, J. Wang, B. Siegel, S. Ghosh, and D. C. Moore, Limits on the abundance of millicharged particles bound to matter, Phys. Rev. D 104, 012004 (2021).
- [22] R. Plestid, V. Takhistov, Y.-D. Tsai, T. Bringmann, A. Kusenko, and M. Pospelov, Constraints on millicharged particles from cosmic-ray production, Phys. Rev. D 102, 115032 (2020).
- [23] H. Wu, E. Hardy, and N. Song, Searching for heavy millicharged particles from the atmosphere, arXiv:2406.01668.
- [24] R. Harnik, R. Plestid, M. Pospelov, and H. Ramani, Millicharged cosmic rays and low recoil detectors, Phys. Rev. D 103, 075029 (2021).
- [25] D. Q. Adams *et al.* (CUORE Collaboration), With or without ν ? Hunting for the seed of the matter-antimatter asymmetry, arXiv:2404.04453.

^[1] R. Millikan and H. Fletcher, Ursachen der scheinbaren unstimmigkeiten zwischen neueren arbeiten uber *e*, Phys. Z. **12**, 161 (1911).

^[2] R. L. Workman *et al.* (Particle Data Group), Review of particle physics, Prog. Theor. Exp. Phys. **2022**, 083C01 (2022).

- [26] C. Alduino *et al.*, The CUORE cryostat: An infrastructure for rare event searches at millikelvin temperatures, Cryogenics 102, 9 (2019).
- [27] E. E. Haller, N. P. Palaio, M. Rodder, W. L. Hansen, and E. Kreysa, NTD germanium: A novel material for low temperature bolometers, in *Neutron Transmutation Doping of Semiconductor Materials* (Springer US, Boston, MA, 1984), pp. 21–36.
- [28] D. Q. Adams *et al.* (CUORE Collaboration), Search for neutrinoless β ⁺EC decay of ¹²⁰Te with CUORE, Phys. Rev. C **105**, 065504 (2022).
- [29] D. Q. Adams *et al.*, Search for double-beta decay of ¹³⁰Te to the 0⁺ states of ¹³⁰Xe with CUORE, Eur. Phys. J. C **81** (2021).
- [30] S. Alvis *et al.* (Majorana Collaboration), First limit on the direct detection of lightly ionizing particles for electric charge as low as e/1000 with the Majorana demonstrator, Phys. Rev. Lett. **120**, 211804 (2018).
- [31] D. Q. Adams *et al.* (CUORE Collaboration), Search for Majorana neutrinos exploiting millikelvin cryogenics with CUORE, Nature (London) **604**, 53 (2022).
- [32] C. Arnaboldi *et al.*, A front-end electronic system for large arrays of bolometers, J. Instrum. 13, P02026 (2018).
- [33] M. Ambrosio *et al.*, Vertical muon intensity measured with MACRO at the Gran Sasso laboratory, Phys. Rev. D **52**, 3793 (1995).
- [34] J. Yocum, D. Mayer, J. Ouellet, and L. Winslow, Muon track reconstruction in a segmented bolometric array using multi-objective optimization, J. Instrum. 17, P07004 (2022).
- [35] S. Banik, V. K. S. Kashyap, M. H. Kelsey, B. Mohanty, and D. H. Wright, Simulation of energy loss of fractionally charged particles using GEANT4, Nucl. Instrum. Methods Phys. Res., Sect. A 971 (2020).
- [36] S. Agostinelli *et al.*, GEANT4–a simulation toolkit, Nucl. Instrum. Methods Phys. Res., Sect. A 506, 250 (2003).
- [37] J. Allison *et al.*, GEANT4 developments and applications, IEEE Trans. Nucl. Sci. **53**, 270 (2006).
- [38] J. Allison et al., Recent developments in GEANT4, Nucl. Instrum. Methods Phys. Res., Sect. A 835, 186 (2016).
- [39] A. Gianvecchio', Synthetic data for the study of the cuore detector response function, J. Phys. Conf. Ser. 2156, 012222 (2021)
- [40] C. Augier *et al.*, Final results on the $0\nu\beta\beta$ decay half-life limit of ¹⁰⁰Mo from the CUPID-Mo experiment, Eur. Phys. J. C **82**, 1033 (2022).
- [41] M. Aglietta *et al.*, Single muon angular distributions observed in the LVD particle astrophysics experiment, Astropart. Phys. **2**, 103 (1994).

- [42] W. Buttinger, Background estimation with the ABCD method, https://indico.cern.ch/event/1122790/contributions/ 4713580/attachments/2381493/4270369/ABCDGuide_ draft18Oct18.pdf.
- [43] F. Abe *et al.* (CDF Collaboration), Measurement of $\sigma b(w \to e \nu)$ and $\sigma b(Z^0 \to e^+ e^-)$ in $\bar{p}p$ collisions at $\sqrt{s} = 1800$ GeV, Phys. Rev. D **44**, 29 (1991).
- [44] G. Aad *et al.*, Search for new phenomena in final states with large jet multiplicities and missing transverse momentum using $\sqrt{s} = 13$ TeV proton-proton collisions recorded by ATLAS in Run 2 of the LHC, J. High Energy Phys. 10 (2020) 062.
- [45] A. Hayrapetyan et al. (CMS Collaboration), Search for soft unclustered energy patterns in proton-proton collisions at 13 TeV, arXiv:2403.05311.
- [46] H. Dembinski, P. Ongmongkolkul *et al.*, scikit-hep/iminuit, 10.5281/zenodo.3949207 (2020).
- [47] F. James and M. Roos, Minuit: A system for function minimization and analysis of the parameter errors and correlations, Comput. Phys. Commun. 10, 343 (1975).
- [48] L. Wasserman, All of Statistics: A Concise Course in Statistical Inference (Springer, New York, 2010), Chap. 15.
- [49] G. Cowan, K. Cranmer, E. Gross, and O. Vitells, Asymptotic formulae for likelihood-based tests of new physics, Eur. Phys. J. C 71, 1554 (2011).
- [50] E. Gross and O. Vitells, Trial factors for the look elsewhere effect in high energy physics, Eur. Phys. J. C 70, 525 (2010).
- [51] D. Baxter *et al.*, Recommended conventions for reporting results from direct dark matter searches, Eur. Phys. J. C 81, 907 (2021).
- [52] M. A. Acero et al., The Profiled Feldman-Cousins technique for confidence interval construction in the presence of nuisance parameters, arXiv:2207.14353.
- [53] G. J. Feldman and R. D. Cousins, Unified approach to the classical statistical analysis of small signals, Phys. Rev. D 57, 3873 (1998).
- [54] A. Lokhov and F. Tkachov, Confidence intervals with a priori parameter bounds, Phys. Part. Nucl. 46, 347 (2015).
- [55] M. Ambrosio *et al.* (MACRO Collaboration), A search for lightly ionizing particles with the MACRO detector, Phys. Rev. D 62, 052003 (2000).
- [56] M. Aglietta *et al.*, Search for fractionally charged particles in the Mont Blanc LSD scintillation detector, Astropart. Phys. 2, 29 (1994).
- [57] M. Mori *et al.*, Search for fractionally charged particles in Kamiokande II, Phys. Rev. D **43**, 2843 (1991).
- [58] I. Alkhatib *et al.* (SuperCDMS Collaboration), Constraints on lightly ionizing particles from CDMSlite, Phys. Rev. Lett. 127, 081802 (2021).
- [59] W. Armstrong *et al.* (The CUPID Interest Group), CUPID pre-CDR, arXiv:1907.09376.